Search for D^0–$\overline{D}^0$ Mixing and Rare Charm Decays

Ulrik Egede, representing the *BABAR* collaboration
Department of Physics, Imperial College London,
London SW7 2AZ, United Kingdom

Based on a dataset acquired by the *BABAR* experiment running on and near the $\Upsilon(4S)$ resonance from 1999-2002, an upper limit is set on the rate of D^0–$\overline{D}^0$ mixing using the decay mode $D^{*+} \to D^0\pi^+$, followed by a semi-leptonic decay of the D^0. Results are compared to previous *BABAR* analysis using hadronic decays. We also set limits on the flavor-changing neutral current decays $D^0 \to e^+e^-$ ($\mu^+\mu^-$) and the lepton-flavor violation decays $D^0 \to e^\pm\mu^\mp$.

1 Overview

The *BABAR* experiment, which is documented in detail elsewhere[1], has since its start in 1999 not only given results on B-physics but also a series of new results in charm physics. With a $c\overline{c}$ cross section of 1.3 nb at the $\Upsilon(4S)$ resonance compared to the cross section of around 1.1 nb for B production there is in fact a higher prompt charm production than B production.

Here we present two new results from *BABAR*. The first one is a search for mixing between the neutral D meson states in the semi-leptonic decay channel[2] while the other is a search for rare lepton decays of the neutral D meson[3]. Both are processes that, if seen with the current statistics, would be clear signs of physics beyond the Standard Model (SM).

2 D^0–$\overline{D}^0$ mixing

Charm mixing is characterised by the two parameters $x \equiv \Delta m/\Gamma$ and $y \equiv \Delta\Gamma/2\Gamma$, where Δm ($\Delta\Gamma$) is the mass (width) difference between the the two neutral D mass eigenstates, and Γ is the average width. We define the overall time-integrated mixing rate as $R_{mix} = (x^2 + y^2)/2$.

Mixing between the neutral charm mesons is, within the SM, heavily suppressed by the GIM mechanism. The expected mixing rate through box and di-penguin diagrams is $\mathcal{O}(10^{-8} - 10^{-10})$ but enhancements involving non-pertubative effects are possible. For a recent review of predictions for both the SM rate and possible New Physics contributions see[4].

To search for mixing the production flavour of the D-meson is tagged from the charge of the pion in the decay $D^{*+} \to D^0\pi^+$ and the decay flavour is tagged from the charge of the electron in the decay $D^0 \to K^-e^+\nu_e$. Charge conjugation is implied everywhere. The decay where the pion and the electron have opposite charge (called the *wrong sign* mode), can only proceed when the D^0 oscillates into a $\overline{D}^0$ before its decay. The *right sign* mode where the pion and electron have the same charge is used as a normalisation mode. In an analysis where the efficiency for right sign and wrong sign decays are identical, R_{mix} is simply given as the time-integrated ratio of the two decay modes.

The analysis is based on a sample of 87 fb^{-1} and uses the $D^0 \to K^-e^+\nu_e$ sample while ignoring the less pure muon sample. The mass difference ΔM between the partially reconstructed D^{*+} candidate and the partially reconstructed D^0 candidate is together with particle identification the main selection criterion to obtain a pure sample.

Separate neural networks, with input parameters specifically describing the D^0 daughters and globally describing the rest of the event, are used to select signal events and reconstruct the D^0 momentum vector. The neural networks, combined with charged kaon and electron particle identification, provide a relatively pure selection of unmixed signal events and give a resolution in ΔM of 2.2 MeV/c^2.

The time distribution of the right sign control sample follows a simple exponential convoluted with a resolution function R, while the wrong sign signal has the form

$$\Gamma_{WS}(t) = e^{-t}\frac{R_{mix}}{2}t^2 \otimes R \ , \tag{1}$$

where t is measured in units of the D^0 lifetime.

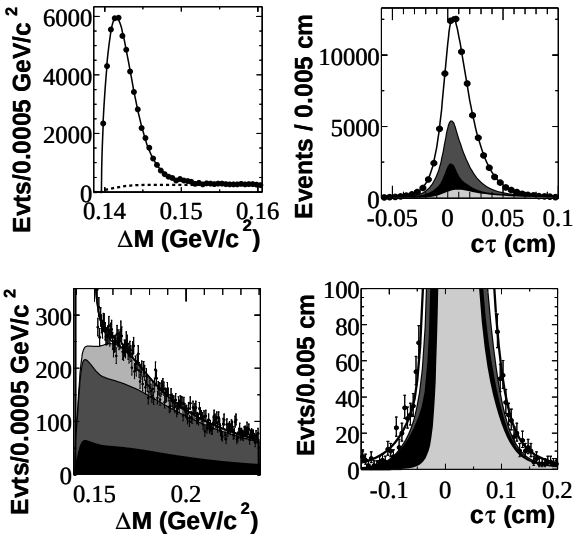

Figure 1: ΔM (left) and decay time (right) projections of fit (solid lines) to RS data (points): (top left) ΔM signal region — unmixed signal (above dashed line), background (dashed line); (bottom left) magnified vertical scale ΔM full fit region — unmixed signal (white), D^+ background (light grey), D^0 background (dark grey), zero-lifetime background (black); (top right) decay time signal region — signal and background components as in bottom left plot; (bottom right) magnified vertical scale decay time full fit region — signal and background components as in bottom left plot of this figure.

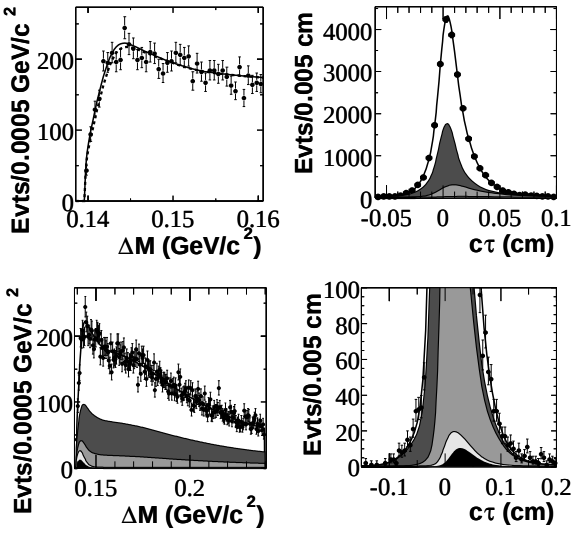

Figure 2: ΔM (left) and decay time (right) projections of fit (solid lines) to WS data (points): (top left) ΔM signal region — mixed signal (above dashed line), background (dashed line); (bottom left) ΔM full fit region — D^0 background (white), zero-lifetime background (dark grey), non-peaking D^+ background (intermediate grey), peaking D^+ background (light grey), mixed signal (black); (top right) decay time signal region — signal and background components as in bottom left plot; (bottom right) magnified vertical scale decay time full fit region — signal and background components as in bottom left plot.

An unbinned extended likelihood fit is performed on the 2-dimensional distribution of signal and background in the variables t and ΔM; first on the right sign sample and then, with the shared parameters between the two datasets constrained, on the wrong sign sample. In Figs. 1 and 2, projections of the fit can be seen overlaid on the data. The result is a wrong sign signal yield of 114 ± 61 events.

Systematic errors arise mainly from the assumptions related to the shape of signal and background in the ΔM variable and when added in quadrature add up to 34% of the statistical error. Combining the wrong sign yield with the right sign yield we get the final result

$$R_{mix} = 0.0023 \pm 0.0012(\text{stat}) \pm 0.0004(\text{syst}) \quad (2)$$

$$R_{mix} < 0.0042 \text{ at } 90\% \text{ CL}. \quad (3)$$

Systematics are taken into account by scaling the log likelihood curve for the fit to the wrong sign yield with the systematic error added in quadrature ($\sqrt{1+0.34^2} = 1.06$). The upper limit was calculated assuming a flat prior for the number of wrong sign events to be positive. In Fig. 3, the result is compared to previous results.

3 Flavour-changing neutral current and lepton-flavour violating decays

In this analysis, a search is performed for the flavour-changing neutral current (FCNC) decays $D^0 \to e^+e^-$ and $D^0 \to \mu^+\mu^-$ and the lepton-flavour violating (LFV) decays $D^0 \to e^\pm\mu^\mp$. In the SM, the FCNC decays are highly suppressed by the GIM mechanism and the LFV decays are strictly forbidden. Compared to rare decay searches in the K and B sector, rare D decays are sensitive to new physics involving the up-quark sector such as certain R-parity violating supersymmetric models[9].

As in the previous analysis the D^0 is required to originate from a D^{*+}, but this time to ensure as clean a sample as possible. For the same reason, the D^0 is required to have a momentum above 2.4 GeV/c in the $\Upsilon(4S)$ centre-of-mass frame to reduce background from combinatorics involving the decay products of B mesons. Electrons (muons) are identified with an efficiency of 95% (60%) with a hadron misidentification probability of 0.2% (2%) as measured on a τ decay control sample.

The decay $D^0 \to \pi^+\pi^-$ is used as a control sample as it has very similar kinematics and, as such, the systematic errors can be minimised. Apart from the particle identification, the selection of the control channel, is identical to the criteria used for the signal.

Based on a sample of 122 fb^{-1} and after optimisation of the selection criteria the events seen in Fig. 4 remain. The background is estimated from the sidebands with a looser selection applied and then scaling it to the final selection taking the small correlation between the criteria into account.

We do not see any signal in any of the channels and the branching fraction upper limits have been calculated using an extension of the Feldman-Cousins method[10] that avoids the unwanted effect of the Feldman-Cousins method[11] that the UL for a search can go down in case of an upwards fluctuation in the expected background. Our result and a comparison to previous published results[12,13] can be seen in Table 1.

References

1. B. Aubert *et al.* [BABAR Collaboration], Nucl. Instrum. Meth. A **479**, 1 (2002).
2. B. Aubert *et al.* [BABAR Collaboration], Accepted by Phys. Rev. D-RC, arXiv:hep-ex/0408066.
3. B. Aubert *et al.* [BABAR Collaboration], Accepted by Phys. Rev. Lett, arXiv:hep-ex/0408023.

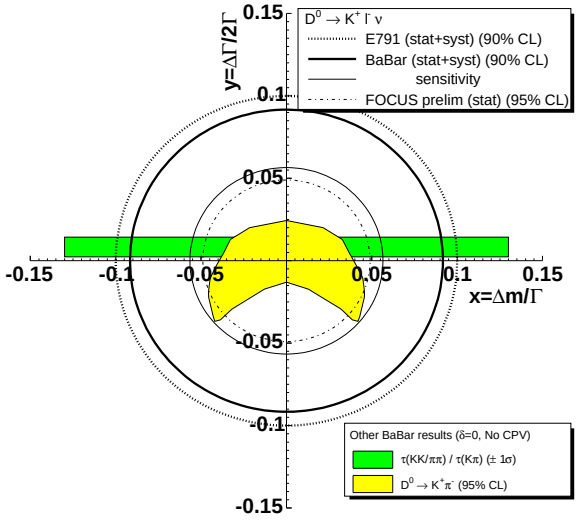

Figure 3: The *BABAR* limit compared to other preliminary and published results using the semi-leptonic decay to search for mixing[5,6]. The thin solid circle shows the sensitivity of the *BABAR* analysis if zero wrong sign signal events were seen. For the comparison to the *BABAR* results from a mixing search with hadronic decays modes[7,8] it is assumed that there is no *CP* violation and that the strong phase difference is zero.

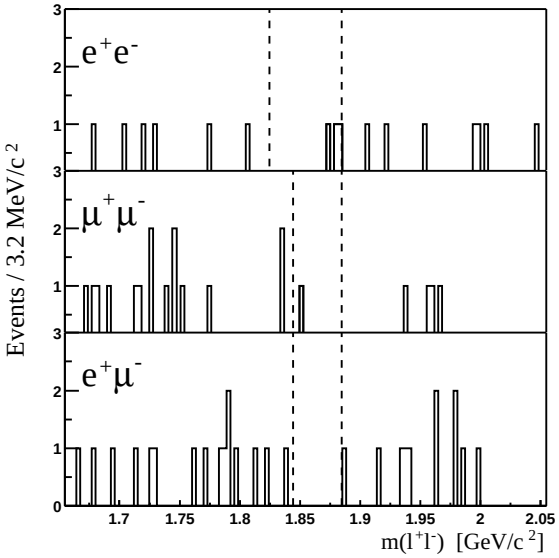

Figure 4: The dilepton invariant mass distribution for each of the decay modes. The dashed lines indicate the optimised signal mass windows.

4. A. A. Petrov, eConf **C030603**, MEC05 (2003) [arXiv:hep-ph/0311371].
5. E. M. Aitala *et al.* [E791 Collaboration], Phys. Rev. Lett. **77**, 2384 (1996)
6. S. Malvezzi [FOCUS Collaboration], ICHEP 2002: Nucl. Phys. B. (Proc. Suppl.) Vol. 117. (April 2003)
7. B. Aubert *et al.* [BABAR Collaboration], Phys. Rev. Lett. **91**, 121801 (2003)
8. B. Aubert *et al.* [BABAR Collaboration], Phys. Rev. Lett. **91**, 171801 (2003)
9. G. Burdman, E. Golowich, J. Hewett and S. Pakvasa, Phys. Rev. D **66**, 014009 (2002).
10. J. Conrad *et al.*, Phys. Rev. D **67**, 012002 (2003).
11. G. J. Feldman and R. D. Cousins, Phys. Rev. D **57**, 3873 (1998).
12. E. M. Aitala *et al.* [E791 Collaboration], Phys. Lett. B **462**, 401 (1999).
13. I. Abt *et al.* [HERA-B Collaboration], Phys. Lett. B **596**, 173 (2004).

	$D^0 \to e^+e^-$	$D^0 \to \mu^+\mu^-$	$D^0 \to e^\pm\mu^\mp$
$N_{\rm bg}^{hh}$	0.02	3.34 ± 0.31	0.21
$N_{\rm bg}^{\rm comb}$	2.21 ± 0.38	1.28 ± 0.32	1.93 ± 0.36
$N_{\rm bg}$	2.23 ± 0.38	4.63 ± 0.45	2.14 ± 0.36
$N_{\rm obs}$	3	1	0
UL at 90% CL	1.2×10^{-6}	1.3×10^{-6}	8.1×10^{-7}
Previous published limit[12,13]	6.2×10^{-6}	2.0×10^{-6}	8.1×10^{-6}

Table 1: The summary of the number of expected background events ($N_{\rm bg}$), number of observed events ($N_{\rm obs}$), and the branching fraction upper limits at the 90 % confidence level for each decay modes. The uncertainties quoted here are total uncertainties. The uncertainty of $N_{\rm bg}^{hh}$ is negligible for the ee and $e\mu$ decay modes.